*SF2A 2013*
*L. Cambrésy, F. Martins, E. Nuss and A. Palacios (eds)*

# SEARCHING FOR PROTOCLUSTERS IN THE FAR–INFRARED WITH HERSCHEL/SPIRE

E. E. Rigby[1], H. J. A. Röttgering[1], N. A. Hatch[2], B. Sibthorpe[3], Y. K. Chiang[4] and R. Overzier[4 5]

**Abstract.** Protoclusters, the high-redshift ancestors of local galaxy clusters, are powerful laboratories for tracing the emergence of large-scale structure, and studying the evolution of galaxies in dense environments. This article presents the results of the first far-infrared, wide-field survey of protoclusters, the ancestors of local galaxy clusters, carried out using the SPIRE instrument on-board the *Herschel* Space Observatory, over the key redshift range $2 < z < 4$.

Examination of the environment within 6 comoving Mpc of the central radio galaxy in each field, reveals that ∼11% of fields contain a $> 3\sigma$ far-infrared excess in source numbers, and there is a tentative trend for the most powerful radio galaxies to host the largest galaxy overdensities. These protocluster candidates are generally contained within 6 comoving Mpc, which is in agreement with simulations and previous work.

Keywords: galaxies, clusters, high–redshift, far–infrared

## 1 Introduction

Studies of protoclusters, the high–redshift seeds of local rich clusters, are an important tool for understanding galaxy and cluster formation during a crucial epoch of their evolution. Historically these overdense structures have been located by targeting luminous high–redshift radio galaxies (HzRGs) as these massive objects are the likely progenitors of Brightest Cluster Galaxies; see Miley & De Breuck (2008) for a review.

Far–infrared observations are a key tool in finding and characterising star–forming protocluster members. They allow the amount of dust–obscured star formation at $2 < z < 4$, when these galaxies build up most of their stellar mass, to be measured by breaking the degeneracy between age and dust content in spectral energy distribution modelling.

The normal field of view of most infra–red or optical instruments is comparable, or even smaller than the angular size of protoclusters ($\sim 10'$), which severely hampers their study. The *Herschel* Space Observatory (Pilbratt et al. 2010)*, with its combination of sensitivity and fast mapping speed, has improved this situation and far–infrared protocluster candidates are beginning to be discovered within the surveys carried out with *Herschel* (e.g. Ivison et al. 2013; Valtchanov et al. 2013, Clements et al. in prep). However, since protoclusters are rare structures the numbers discovered in this way are likely to be low.

This article presents the results of a targeted, survey of 26 HzRG fields that uses the Spectral and Photometric Imaging REciever (SPIRE; Griffin et al. 2010) on–board *Herschel* to map an area sufficient to encompass the full protocluster extent, together with its surrounding environment. For further details see Rigby et al. (2013). Throughout this article a concordance cosmology is assumed, with values for the cosmological parameters of $H_0 = 71$ km s$^{-1}$Mpc$^{-1}$, $\Omega_m = 0.27$ and $\Omega_\Lambda = 0.73$. This gives a physical scale at $z = 2$ of 8.475 kpc/$''$ and 7.083 kpc/$''$ at $z = 4$. These correspond to ∼1.5 comoving Mpc/$'$ and ∼2.1 comoving Mpc/$'$ respectively.

[1] Leiden Observatory, P.O. Box 9513, 2300 RA, Leiden, The Netherlands
[2] School of Physics and Astronomy, University of Nottingham, University Park, Nottingham NG7 2RD, UK
[3] SRON Netherlands Institute for Space Research, Landleven 12, 9747 AD, Groningen, The Netherland
[4] Department of Astronomy, The University of Texas at Austin, Austin, TX 78712
[5] Observatório Nacional, Rua José Cristino, 77. CEP 20921-400, São Cristóvão, Rio de Janeiro-RJ, Brazil

*Herschel is an ESA space observatory with science instruments provided by European-led Principal Investigator consortia and with important participation from NASA.

## 2 The *Herschel* protocluster survey

The 26 HzRGs selected for this work have $L_{500\mathrm{MHz}} > 10^{28.5}$ W Hz$^{-1}$ and are evenly spread across $2 < z < 4$. Eight are known protoclusters, identified via previous Ly$\alpha$ or H$\alpha$ observations. They were observed at 250, 350 and 500 $\mu$m with SPIRE, and the resulting maps cover areas of 400 – 900 arcmin$^2$.

The SPIRE data were reduced using the standard *Herschel* pipeline and individual catalogues for each of the 3 bands were created using the STARFINDER algorithm (Diolaiti et al. 2000). These were then combined, using the 500 $\mu$m catalogue as a prior, to create a matched catalogue for each field. Of the 26 original fields, 7 were excluded from the subsequent analysis as they were contaminated by galactic cirrus. Full details of the data reduction and source extraction can be found in Rigby et al. (2013).

### 2.1 High–redshift selection

Before searching for potential protocluster–related overdensities in the far–infrared data it is useful to impose a cut to select sources which lie near the redshift of the HzRG in each field. A simple colour cut ($f_{350\mu m}/f_{250\mu m} \geq 0.85$ for instance) will select sources with $z \gtrsim 2$ (e.g. Amblard et al. 2010), but, since the HzRGs cover $2 < z \lesssim 4$, contaminating foreground galaxies will still remain in a large proportion of the fields. A more sophisticated approach is to use a custom–colour selection, tailored to the redshift of each HzRG; this technique is illustrated in Figure 1. This allows the search to be restricted to sources with estimated redshifts within $\pm 0.2(1+z)$ of the HzRG only.

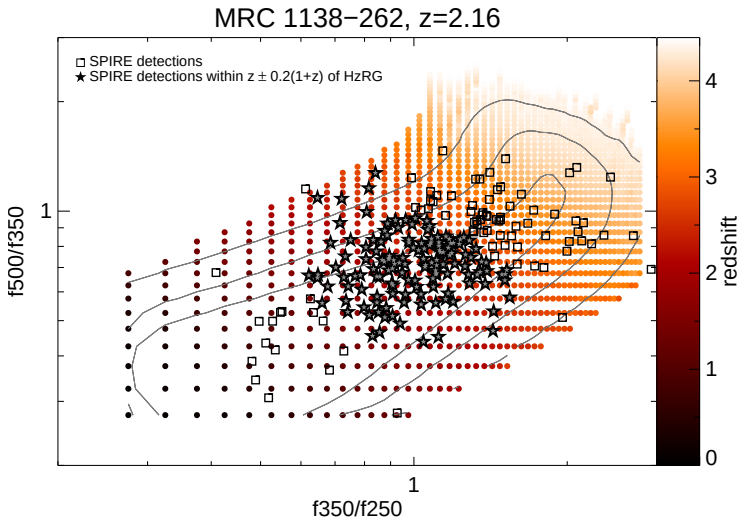


**Fig. 1.** SPIRE colour–colour diagram for one of the HzRG fields, illustrating the custom–colour redshift selection. Catalogue sources are selected to lie within $\pm 0.2(1+z)$ of the redshift of the HzRG by comparing their SPIRE colours with those of an artificially redshifted galaxy template (constructed following Roseboom et al. 2012). Stars and squares indicate sources selected and rejected as potential protocluster members respectively; solid points show the colour track of the template galaxy, broadened by a Gaussian uncertainty of 10%, as it evolves in redshift. Lines show the 1, 2 and 3$\sigma$ contours in the template distribution.

## 3 Surface density analysis

After applying the custom colour redshift selection to each field the galaxy surface density is calculated by counting the number of sources within 6 comoving Mpc of the HzRG position. A reference field, drawn from the SPIRE archive, is used to determine the surface density of background galaxies for comparison, after applying the same colour selections. Figure 2 shows the results, plotted against the redshift and radio luminosity of the central HzRGs. Of the 19 fields, 2 are $> 3\sigma$ overdense and both are not previously known protoclusters (only 1 of the known protoclusters shows signs of an overdensity, but only at the $2\sigma$ level). Larger overdensities tend to

lie at $L_{500\mathrm{MHz}} \gtrsim 10^{29}$ and $z < 3$, but there are no definite trends with either parameter. However, this apparent preference for brighter HzRGs is consistent with previous work Galametz et al. (2012, and references therein).

The 2 fields with the strongest overdensities are detected at the 3.9 and 4.3$\sigma$ level respectively. The probability of finding 2 $\geq 3\sigma$ overdensities such as these by chance, given that 19 fields were observed is $5 \times 10^{-4}$. These results, therefore, are inconsistent with being due to random background fluctuations.

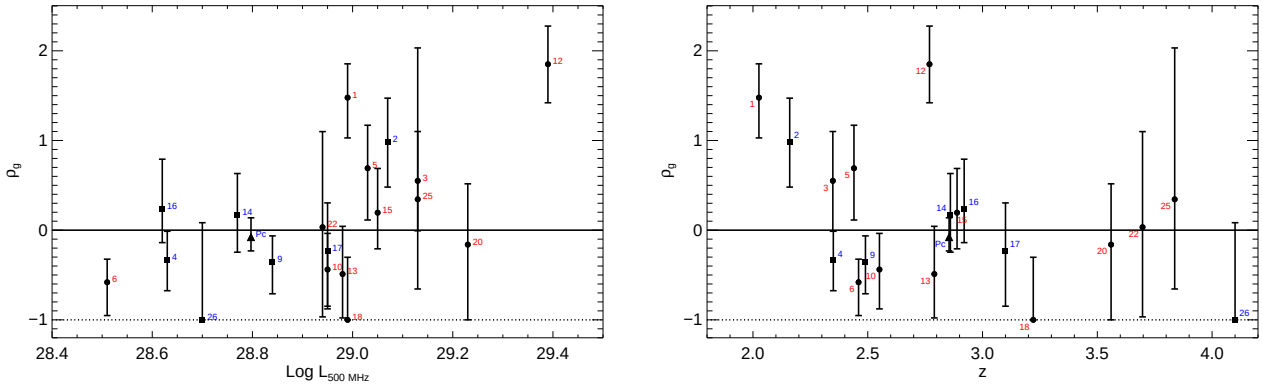


**Fig. 2. Left:** The overdensity of galaxies in each field as a function of radio power of the central HzRG. This is defined as $\rho_{\mathrm{g}} = (\rho_{\mathrm{obs}} - \rho_{\mathrm{bkg}})/\rho_{\mathrm{bkg}}$ where $\rho_{\mathrm{obs}}$ and $\rho_{\mathrm{bkg}}$ are the observed surface density and mean background surface density respectively. **Right:** The overdensity of galaxies in each field as a function of redshift of the central HzRG. In both cases galaxies are colour–selected from the matched catalogue and counted within a radius of 6 comoving Mpc and $\pm 0.2(1+z)$ of the position and redshift of the HzRG; only the 19 low–cirrus fields are considered. Numbers correspond to the field labels. Blue colours and square symbols highlight the 7 known protoclusters, and the average overdensity of these fields is labelled 'Pc'. A value of $\rho_{\mathrm{g}} = -1$ (indicated by the horizontal dotted line) corresponds to a field containing no galaxies which satisfied the position and redshift criteria.

## 4 Are the overdensities consistent with HzRG-centred protoclusters?

A simple characterisation of the galaxy overdensities seen here can be found by comparing them to protocluster predictions from cosmological simulations. Chiang et al. (in prep) follow the evolution with redshift of $\sim 3000$ clusters in the Millennium Simulation (Springel et al. 2005; Guo et al. 2011), and can therefore match the properties of a local massive cluster to the high–redshift protocluster it grew from. This is compared to the *Herschel* results by applying a redshift–dependent cut in star–formation rate ($SFR \geq c10^{0.2z}$ $\mathrm{M}_{\odot}$/yr), assuming that the detected galaxies mirror the highest rank of SFR in the simulated galaxy population at a given redshift.

Figure 3 shows the variation in the number of member galaxies with radial extent for three separate bins in simulated cluster mass (defined at $z = 0$). Also shown is the position of the average $\geq 3\sigma$ galaxy overdensities seen in the *Herschel* data; this implies an enclosed mass for these structures of $> 10^{14}$ $\mathrm{M}_{\odot}$, which is consistent with that determined previously for HzRG–selected protoclusters (e.g. Venemans et al. 2007; Hatch et al. 2011). However, it should be noted that the large redshift range searched means that contamination of the overdensity from foreground and background galaxies is likely. Firm confirmation of the galaxy excesses seen here can only be done by reducing the redshift uncertainty.

## 5 Summary and Conclusions

Investigating the far–infrared environments surrounding 19 HzRGs has revealed significant galaxy overdensities in 2 fields. These are unlikely to be due to random background fluctuations and are consistent with simulated protoclusters of mass $> 10^{14}$ $\mathrm{M}_{\odot}$.

The surface density of these fields at these wavelengths is generally low, which must in part be due to the large SPIRE beam making overdensities hard to identify here. Overall these results demonstrate that *Herschel* has the potential to identify protocluster candidates, but that this is a less successful technique here than at other wavelengths. It is likely that SPIRE is probing different structures than those identified using classical

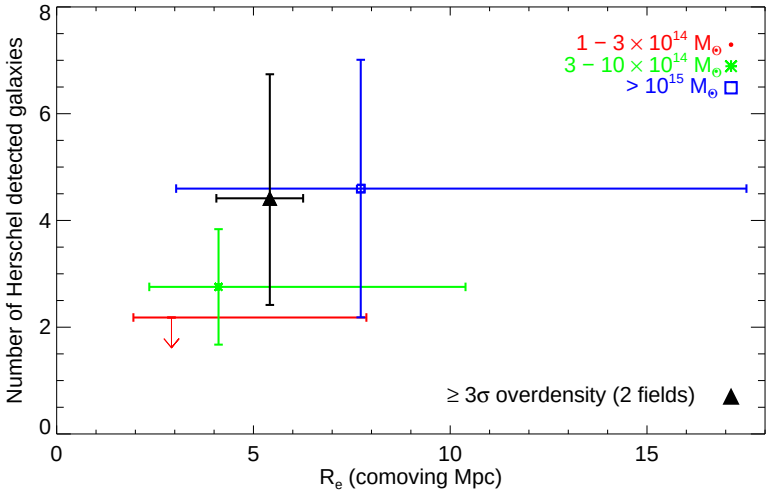


**Fig. 3.** The number of galaxies contained within simulated protoclusters as a function of their radial extent, for 3 different bins in descendent (i.e. $z = 0$) mass (coloured points). The black triangle shows the average size and number of galaxies of the $\geq 3\sigma$ overdensities in the *Herschel* sample. The uncertainties on the simulated points represent the spread in the simulated distribution; the uncertainties on the real data point come from the spread in the radial extent calculation.

narrow–band or mid–infrared imaging. Future work will combine these SPIRE data with forthcoming radio imaging to improve the selection of protocluster member galaxies, and understand the different far–infrared populations.

## References

Amblard, A., et al. 2010, A&A, 518, L9
Diolaiti, E., Bendinelli, O., Bonaccini, D., et al. 2000, Proc. SPIE, 4007, 879
Galametz, A., Stern, D., De Breuck, C., et al. 2012, ApJ, 749, 169
Griffin, M. J., et al. 2010, A&A, 518, L3
Guo, Q., White, S., Boylan-Kolchin, M., et al. 2011, MNRAS, 413, 101
Hatch, N. A., De Breuck, C., Galametz, A., et al. 2011a, MNRAS, 410, 1537
Ivison, R. J., Swinbank, A. M., Smail, I., et al. 2013, arXiv:1302.4436
Miley, G., & De Breuck, C. 2008, A&A Rev., 15, 67
Pilbratt, G. L., et al. 2010, A&A, 518, L1
Roseboom, I. G., Ivison, R. J., Greve, T. R., et al. 2012, MNRAS, 419, 2758
Rigby, E. E., Hatch, N. A., Röttgering, H. J. A. et al. 2013, MNRASsubmitted
Springel, V., White, S. D. M., Jenkins, A., et al. 2005, Nature, 435, 629
Valtchanov, I., Altieri, B., Berta, S., et al. 2013, arXiv:1309.4223
Venemans, B. P., Röttgering, H. J. A., Miley, G. K., et al. 2007, A&A, 461, 823